Article

Flexible Furfural-Based Barrier Polyester from a Self-Condensable Monomer

Asmaa M. Ahmed, Tuomo P. Kainulainen, Juho Antti Sirviö, and Juha P. Heiskanen*

Read Online

ACCESS | Metrics & More | Article Recommendations | Supporting Information

ABSTRACT: A novel biobased sulfur-bridged polyester, with high oxygen barrier properties, was synthesized via self-condensation of a new AB-type furfural-based monomer, i.e., methyl 5-[(2-hydroxyethyl)sulfanyl]furan-2-carboxylate (MSF). The novel MSF-based polyester (pMSF) showed a 15× higher barrier improvement factor compared to amorphous poly(ethylene terephthalate) (PET) and good UV light filtering, with a cutoff wavelength of ca. 340 nm, thanks to the introduced sulfur heteroatom. Interestingly, pMSF offers a circular life cycle, with excellent chemical recyclability. Furthermore, the new self-condensable monomer, MSF, was utilized as a comonomer to improve the O_2 barrier performance of poly(ethylene furanoate) (PEF) and poly(ethylene bifuranoate) (PEBF). The new copolymers, i.e., $PEF_{80}MSF_{20}$ and $PEBF_{80}MSF_{20}$, have been characterized by structural, thermal, mechanical, and barrier measurements. The results clearly show that the novel monomer, MSF, is a promising precursor for sustainable biobased packaging materials with benefits of high O_2 barrier, UV light filtering, flexibility, and chemical recyclability.
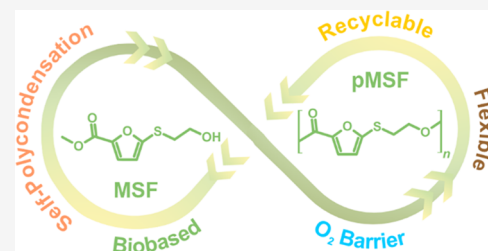
INTRODUCTION

There is a critical need for realizing a biobased materials economy due to climate change and the environmental consequences of global plastic pollution. Among possible renewable polymer candidates, poly(ethylene furanoate) (PEF), potentially derived from cellulose, has attracted much attention due to its promising attributes for eco-friendly barrier packaging applications.[1−6] Because of its better sustainability and superior performance, PEF is deemed to become another important commodity polymer competing with petroleum-based poly(ethylene terephthalate) (PET). When compared against PET, the O_2 and CO_2 barrier improvement factors (BIFs) of PEF were about 5.5−11 and 11−19, respectively (Figure 1).[7,8] This superior barrier performance is attributed to the hindered ring flipping and low segment mobility induced by the PEF's heteroaromatic 2,5-furandicarboxylate (FDCA) backbone unit.[9,10]

Clearly, the different chemical functionality of biomass-derived monomers can endow the resulting polymers with high performance. Thus, considerable attention has been focused on engineering other furan-based polymers via versatile biobased monomers. The development and application of such biobased monomers not only deliver sustainable alternatives for conventional petroleum-based polyesters but also offer insights into the development of new polyesters. For instance, the hemicellulose-based monomer dimethyl 2,2′-bifuran-5,5′-dicarboxylate (dm-BFDCA),[11−14] which is a dimeric analogue of dm-FDCA, was utilized as a precursor for poly(ethylene 2,2′-bifuranoate) (PEBF) (Figure 1). PEBF had about 4.2× lower O_2 permeability, compared to PET, and provided UV light blocking at long wavelengths (up to 400 nm). The highly

conjugated heteroaromatic moiety ensured a higher glass transition temperature ($T_g \sim 107$ °C) over that of PEF ($T_g \sim 85$ °C).[14,15]

Recently, we reported polyesters derived from hemicellulose-based dimethyl 5,5′-sulfanediyldifuranoate (dm-SFA), where a sulfur atom was utilized as a bridge between two furan rings.[16] Poly(ethylene sulfanediyldifuranoate) (PESF), for example, showed excellent O_2 barrier performance with BIF = 11.2 compared to PET (Figure 1). In contrast to the semicrystalline PEF and PEBF, PESF displayed an amorphous character. Its UV light cutoff was intermediate between PEF and PEBF.[16]

Based on our previous good results with the SFA monomer and the resulting homopolyesters such as PESF,[16] we now designed a novel monomer, methyl 5-[(2-hydroxyethyl)-sulfanyl]furan-2-carboxylate (MSF), where the sulfur heteroatom links together a biomass-derived methyl furoate structure and a hydroxyethyl chain. Due to its AB-type functionality, it was deduced to provide polyester(s) via self-condensation in a similar fashion to phenyl-derived AB-type monomers.[17−21] Conversely, the resulting polymer was expected to have easy recyclability. Here, we will demonstrate the synthesis of MSF, the homopolyester derived from MSF,
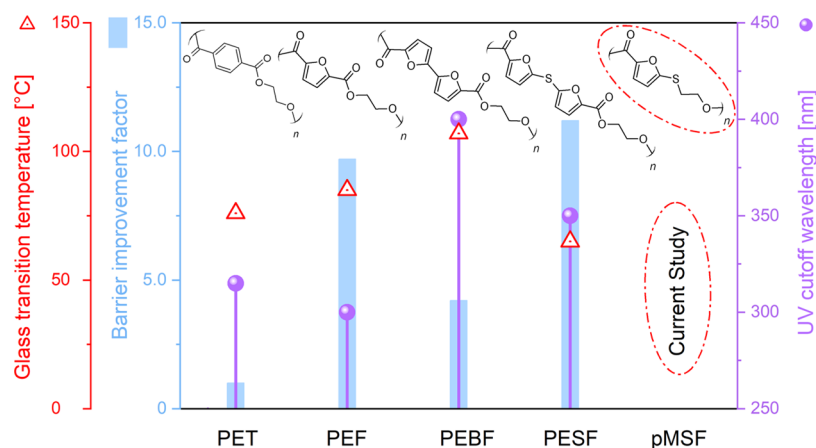
Figure 1. Key properties of the relevant polyesters.

and copolyesters of PEF and PEBF incorporating MSF. Intriguingly, MSF appears to be a useful monomer/comonomer for the synthesis of low O_2 permeability polyesters.

■ EXPERIMENTAL SECTION

Materials. *N,N*-Dimethylformamide (DMF, 99.8%), 2-mercaptoethanol (ME, ≥99%), tetrabutyl titanate (TBT, 99%), ethylene glycol (EG, 99.8%), methyl 5-bromofuran-2-carboxylate (99%), other commercially available chemicals, and solvents were used as received unless otherwise noted. Dimethyl 2,5-furandicarboxylate (dm-FDCA) and dimethyl 2,2′-bifuran-5,5′-dicarboxylate (dm-BFDCA) were synthesized according to previous reports.[22,23] Thin-layer chromatography (TLC) was used for monitoring reactions using an ethyl acetate/hexane mixture as an eluent. ^{13}C NMR measurements of the polymer samples were performed with 16000 scans.

Syntheses. *Monomer Synthesis. Methyl 5-[(2-Hydroxyethyl)-sulfanyl]furan-2-carboxylate (MSF).* Methyl 5-bromofuran-2-carboxylate (10 mmol, 2.05 g) and K_2CO_3 (1 equiv, 1.39 g) were mixed with DMF (10 mL) in a 50 mL round-bottom flask. ME (1 equiv, 0.70 mL) was added dropwise to the reaction flask under an argon gas stream. The reaction flask was sealed, and the reaction mixture was stirred at room temperature (19−20 °C) for 24 h. After dilution with deionized water (50 mL), the organic layer was extracted with ethyl acetate (3 × 50 mL) and dried over anhydrous $MgSO_4$. The crude product was purified by column chromatography using a gradient elution of toluene/ethyl acetate mixtures to afford the monomer as a colorless viscous liquid (1.88 g, 89%). ^1H NMR (400 MHz, $(CD_3)_2SO$, ppm): δ 7.32 (d, *J* = 3.5 Hz, 1H), 6.74 (d, *J* = 3.5 Hz, 1H), 5.00 (t, *J* = 5.6 Hz, 1H), 3.80 (s, 3H), 3.57 (q, *J* = 6.2 Hz, 2H), 3.02 (t, *J* = 6.5 Hz, 2H). ^1H NMR (400 MHz, $CDCl_3$, ppm): δ 7.15 (d, *J* = 3.6 Hz, 1H), 6.55 (d, *J* = 3.6 Hz, 1H), 3.89 (s, 3H), 3.81 (t, *J* = 6.0 Hz, 2H), 3.10 (t, *J* = 6.0 Hz, 2H), 2.41 (s, 1H).

^{13}C NMR (101 MHz, $(CD_3)_2SO$, ppm): δ 157.9, 152.3, 145.0, 120.2, 115.2, 60.1, 52.0, 36.7. ^{13}C NMR (101 MHz, $CDCl_3$, ppm): δ 158.5, 150.9, 146.2, 119.4, 116.5, 61.1, 52.0, 37.7. HRMS (*m/z*) (ESI$^+$) calcd for $C_8H_{10}O_4SNa$ [M + Na]$^+$: 225.0192, Found 225.0192.

Polymerization Procedures. Two different techniques were adopted to polymerize MSF in the presence of the TBT catalyst. The first comprised polycondensation under atmospheric pressure and the use of a high-boiling-point solvent along with molecular sieves as a drying agent. The second technique consists of two steps, i.e., transesterification under atmospheric pressure followed by polycondensation under vacuum. Both procedures are detailed below.

Polycondensation of MSF under Atmospheric Pressure. MSF (6.32 mmol, 1.28 g) was mixed with TBT (0.1 mol % equiv, 2.33 mg) and 10 mL of toluene (dried over 4 Å molecular sieves) in a 50 mL round-bottom flask. A tube filled with 25 g of 4 Å molecular sieves was connected on top, followed by a condenser and an argon gas inlet.

The reaction system was evacuated and filled with argon gas for 5 cycles. The polycondensation was carried out under argon by heating the flask at 170 °C for 1 h and continuing at 180 °C for 11 h. The observed viscosity of the reaction mixture was dramatically increased in the first 3 h. The solid reaction product was dissolved in 10 mL of chloroform at 40 °C. The polymer was precipitated and washed using cold methanol and then collected by filtration. Finally, drying under vacuum at 50 °C afforded pMSF as a white-to-off-white clump (1.16 g, 98%). ^1H NMR (400 MHz, $CDCl_3$, ppm): δ 7.13 (d, *J* = 3.4 Hz, 1H), 6.60 (d, *J* = 3.4 Hz, 1H), 4.49 (t, *J* = 6.6 Hz, 2H), 3.25 (t, *J* = 6.6 Hz, 2H). ^{13}C NMR (101 MHz, $CDCl_3$, ppm): δ 157.5, 150.9, 145.9, 119.9, 116.7, 63.2, 32.9.

Polycondensation of MSF under Vacuum. MSF (9 mmol, 1.87 g) and TBT (0.1 mol % equiv, 3.2 mg) were placed in a 50 mL flask equipped with a distillation bridge, receiving flask, and argon gas inlet. Five vacuum−argon cycles were carried out prior to the reaction. The transesterification step was started by heating the flask to 170−180 °C and continued for 2.5 h under argon. The polycondensation step was then started by gradually reducing the pressure to 0.2 mbar and raising the reaction temperature to 200 °C for 2 h. Because of the low pressure, evaporation of free monomer and oligomer(s) took place, resulting in condensate formation on the flask walls. The polymer was acquired as a white powder after dissolution in 5 mL of chloroform and precipitation in excess methanol, as done previously. The precipitated polymer was filtered and dried under ambient conditions to yield a white polymer powder (0.66 g, 42%).

Synthesis of Copolymers. The prepared copolyesters are coded as PEF$_{80}$MSF$_{20}$ and PEBF$_{80}$MSF$_{20}$, where the molar fraction of FDCA or BFDCA was 0.8, and that of MSF was 0.2. The previously described two-stage polycondensation procedure was followed to synthesize the target copolymers. Ethylene glycol (3−5 equiv, 0.99−1.67 mL), MSF (0.25 equiv, 0.303 g), and TBT (0.1 mol %, 2.01 mg dissolved in 1 mL of toluene) were placed in a 50 mL round-bottom flask. The liquid reactants were first mixed under argon stream, and then dm-FDCA (6 mmol, 1.10 g) or dm-BFDCA (6 mmol, 1.50 g) was added to the reaction flask. The transesterification step was performed at 180−200 °C for 4 h under argon atmosphere, followed by the polycondensation step at 240 °C under 0.4−0.1 mbar pressure for another 4 h. The polyesters were dissolved in 12 mL of HFIP/CHCl$_3$ (1:3 v/v) and precipitated in cold methanol to yield off-white fibers. The copolymer fibers were filtered, washed with methanol, and dried under vacuum at 50 °C to a constant weight to give either PEF$_{80}$MSF$_{20}$ (1.17 g, 90%) or PEBF$_{80}$MSF$_{20}$ (1.7 g, 93%). For NMR analysis, PEF$_{80}$MSF$_{20}$ was dissolved in $CDCl_3$, while PEBF$_{80}$MSF$_{20}$ required a mixture of $CDCl_3/CF_3COOD$ (10:1 v/v) for dissolution.

PEF$_{80}$MSF$_{20}$: ^1H NMR (400 MHz, $CDCl_3$, ppm): δ 7.24 (s, 2H), 7.20 (d, *J* = 3.5 Hz, 1H) 6.6 (d, *J* = 3.5 Hz, 1H), 4.66 (s, 4H), 4.53 (t, *J* = 6.4 Hz, 2H), 3.26 (t, *J* = 6.4 Hz, 2H). ^{13}C NMR (101 MHz, $CDCl_3$, ppm): δ 157.5, 150.7, 146.4, 120.0, 119.0, 116.8, 68.8, 62.8, 32.8.

Scheme 1. Synthesis Route for the MSF Monomer and the Corresponding Polyester pMSF
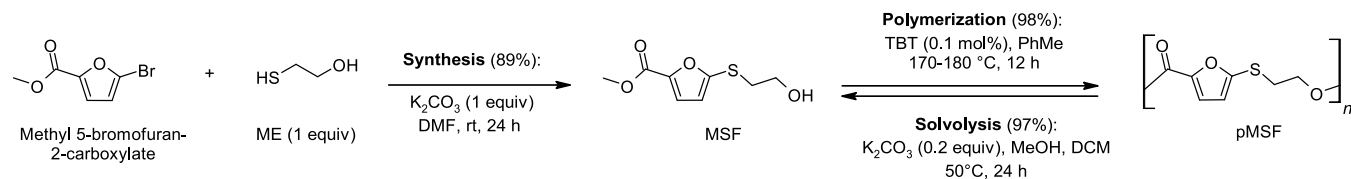
PEBF$_{80}$MSF$_{20}$: ^{1}H NMR (400 MHz, CDCl$_3$, ppm): δ 7.40 (d, J = 3.7 Hz, 2H), 7.34 (d, J = 3.6 Hz, 1H), 6.94 (d, J = 3.7 Hz, 2H), 6.61 (d, J = 3.6 Hz, 1H), 4.77 (s, 4H), 4.59 (t, J = 6.4 Hz, 2H), 3.33 (t, J = 6.4 Hz, 2H). ^{13}C NMR (101 MHz, CDCl$_3$, ppm): δ 160.7, 160.3, 153.0, 149.2, 144.4, 142.9, 121.9, 116.2, 110.3, 64.5, 63.6, 31.9.

Chemical Recyclability. MSF was recovered via the solvolysis of pMSF according to a previously reported procedure for PET.[24] The pMSF film pieces (1 mmol of repeating units, 170.2 mg), K$_2$CO$_3$ (0.2 equiv, 27.6 mg), methanol (50 equiv, 2 mL), and dichloromethane (16 equiv, 1 mL) were mixed in a sealed 10 mL tube at 50 °C for 24 h. After cooling, the reaction solution was diluted with ethyl acetate and filtered through a silica gel layer. The pure monomer was recovered after solvent evaporation (196.4 mg, 97%).

In another trial, methanol was employed as the only solvent, using the same molar ratios as in the previous experiment. After solvolysis at 50 °C for 24 h, the reaction solution was diluted with 2 mL of deionized water, and the organic layer was extracted with ethyl acetate (3 × 10 mL) and dried over anhydrous MgSO$_4$. MSF was recovered after solvent evaporation (59.9 mg, 79%). The aqueous layer was acidified (pH 1−2) with 37% HCl, and the precipitated powder was filtered and dried to afford the acid form of MSF as a white powder (30.4 mg, 15%). ^{1}H NMR (400 MHz, CDCl$_3$, ppm): δ 7.29 (d, J = 3.6 Hz, 1H), 6.58 (d, J = 3.6 Hz, 1H), 3.86 (t, J = 6.0 Hz, 2H), 3.16 (t, J = 6.0 Hz, 2H), 2.15 (s, 1H).

Copolymers were depolymerized into their corresponding monomers using the previously discussed solvolysis procedure.[24] The methanol solvolysis of PEF$_{80}$MSF$_{20}$ (1 mmol of repeating units, 179.7 mg) afforded a mixture of monomers (221.4 mg) containing dm-FDCA (76%) and MSF (24%). The solvolysis of PEBF$_{80}$MSF$_{20}$ (1 mmol of repeating units, 232.6 mg) using a methanol/dichloromethane solvent mix afforded a mixture of monomers (228.2 mg) including dm-BFDCA (81%) and MSF (19%).

Characterization. *Dilute Solution Viscometry.* Intrinsic viscosities (IVs) of the prepared polymers were recorded using a micro-Ubbelohde viscometer and a solvent mixture of phenol and 1,1,2,2-tetrachloroethane (60:40, w/w) at 30.0 °C. The polymer solution was prepared at the concentration of 0.50 g/dL, and the average of three flow times of solvent mixture (t_0) and polyester solutions (t) were used to calculate the relative viscosities ($\eta_r = t/t_0$). The IVs values were calculated using the Billmeyer equation: $[\eta] = [0.25 \times (\eta_r - 1 + 3 \times \ln \eta_r)]/c$.[25]

Differential Scanning Calorimetry (DSC). A Mettler Toledo DSC 821e was used to investigate the thermal behavior of polyester in the range of −20−200 °C under N$_2$ gas flow (50 cm^3/min) with heating and cooling rates of 10 °C/min. For the copolymers, heating−cooling scans in the range of 20−250 °C were used.

Thermogravimetric Analysis (TGA). Netzsch STA 409 was used to evaluate the thermal stability and decomposition properties of pMSF and its copolymers in the heating range of 38−700 °C, under air or nitrogen, using a gas flow rate of 20 cm^3/min and a heating rate of 10 °C/min.

Film Processing. A hydraulic press (Fontijne LabEcon 300) was used to acquire melt-pressed films. The dried polymer sample (ca. 1 g) was placed between preheated two aluminum plates (20 cm × 20 cm) covered with, commercially available, PTFE-coated glass fiber sheet with a thickness of 140 μm (216.15CF, Fiberflon Gmbh & Co. KG). A square frame of the same glass fiber was placed around the plates to control the thickness of the pressed film. The pMSF sample was melted at 150 °C for 3 min, and copolymers PEF$_{80}$MSF$_{20}$ and PEBF$_{80}$MSF$_{20}$ were processed at temperatures of 180 and 230 °C,

respectively, then pressed for 2 min at 30 and 50 kN. The plates were cooled under the applied pressure using the water-cooling circuit of the press. Then, the aluminum plates were separated, and the films were peeled off carefully to yield flexible and transparent films. NMR measurements of the melt-pressed film samples showed that no degradation occurred during processing. PET, PEF, and PESF were previously prepared by our group according to the same protocol and were used as reference films. Commercial PET pellets were used to prepare the amorphous PET films.[16,26] PEBF was prepared by our team and others and processed under quite similar conditions.[14,15] Thickness gauge (Precision Thickness Gauge FT3, Hanatek Instrument, UK) was used to measure the exact thickness of polymer film samples used for characterization.

Tensile Testing. Rectangle-shaped specimens of polyester films with 5 mm width and thicknesses between 50 and 200 μm were stored under ambient conditions (23 °C, 50% RH) for 48 h before the tests. Tensile testing was carried out under the same conditions by means of a tensile tester (Zwick Roell 2.5 kN) using a gauge length of 30 mm and a crosshead speed of 5 mm/min. The reported mechanical results were obtained from five measurements. The elastic deformation test of pMSF was performed using a film of 5.0 mm width and 70 μm thickness. The sample specimen was preloaded to a strain of 200% using a crosshead speed of 20 mm/min for 1 min, and then the clamps began to return at the same speed until no more tension force was recorded on the sample. The pMSF specimen was allowed to return to its original shape for 48 h.

Dynamic Mechanical Analysis (DMA). Storage modulus E', loss modulus E'', and tan δ were evaluated from rectangular-shaped polymer specimens using a DMA Q800 (TA Instruments). A "multifrequency, strain" mode was used at 1 Hz, 0.08% strain at a heating rate of 3 °C/min from −50 to 120 °C and from −50 to 200 °C for pMSF and the copolyesters, respectively.

Gas Permeability Analysis. MOCON OxTran 2/20 was used to measure the oxygen permeability (OP) of the melt-pressed polyester films as well as reference PET films at 23 °C and 0% RH (relative humidity) with a specimen exposure area of 5 cm^2. OP values were measured from samples of melt-pressed films with thicknesses of 50−200 μm. The value of the barrier improvement factor was calculated by dividing the OP value of reference PET films by that of polyester. The OP of reference films PET, PEF, and PESF were measured according to the same procedure.[16,26] The OP of PEBF was measured by another team under similar conditions of 23 °C and 0% RH.[15]

UV−Vis. A Shimadzu UV-1800 spectrophotometer was used to acquire transmission spectra of thin rectangle-shaped film pieces in the wavelength range of 200−800 nm.

RESULTS AND DISCUSSION

Monomer Synthesis. Due to their nucleophilicity, thiols are often applied in reactions for the formation of a C−S bond. 2-Mercaptoethanol was utilized here to produce the desired sulfur bridge between the furan ring and the aliphatic chain to obtain the requisite monomer MSF (Scheme 1). The chemical structure of the synthesized monomer was validated by NMR and HRMS analyses (Figures S1−S3 in the Supporting Information). Contrary to some of the reported phenyl-derived AB-type monomers with cyclic structure,[17,19−21] MSF exists as an acyclic monomer due to its 2,5-substitution pattern of furan ring. The alcohol group of ME conveniently provides the required functionality for self-condensation, as well. Since

methyl 5-bromofuran-2-carboxylate was used as the furan precursor, the methyl ester group then provided the second required moiety for self-condensation. Reaction conditions were optimized by varying the solvent, molar equivalents of ME and of K_2CO_3, reaction temperature, and time. Among the different solvents that were tested, i.e., DMF, DMA, acetonitrile, dioxane, chloroform, methanol, and ethyl acetate, only DMF gave full conversion to MSF. Moreover, the monomer yield was highest (97%) when the higher molar ratio of ME, up to 1.5 equiv, was used. However, excess ME favored side reactions and tended to form a disulfide byproduct under the basic conditions. Separating the monomer, residual ME, and disulfide was problematic since MSF and the impurities are not easily separated, even by vacuum distillation. It is also worth mentioning that the removal of impurities containing hydroxyl or ester groups is required; they will otherwise hinder the desired polymerization of MSF. To our satisfaction, the desired monomer was still produced in 89% yield when ME was used in a 1:1 molar ratio to methyl 5-bromofuran-2-carboxylate. Recovery of the unreacted furan starting material was undoubtedly more convenient and simpler. Furthermore, the molar ratio of the base affected the resulting crude product. The dimeric structure and short oligomers were detected in crude MSF when the molar amount of K_2CO_3 was higher than other reactants. Similarly, a longer reaction time and/or higher temperature resulted in slight self-condensation. The optimal result was obtained when the reaction was carried out with a 1:1:1 molar mixture of methyl 5-bromofuran-2-carboxylate, ME, and K_2CO_3 in DMF at 20 °C for 24 h.

Polymer Synthesis. To obtain the desired homopolyester (pMSF), self-condensation of MSF was attempted with TBT as a catalyst. Under typical high-vacuum polycondensation conditions, MSF appeared to polymerize, but simultaneous sublimation was observed, i.e., a ring of wet crystals formed on the upper parts of the reaction flask. According to ^{1}H NMR analysis, the condensate contained both MSF and a solid cyclic oligomer (Figure S4). Since the requirement for polycondensation in this system is the removal of the released methanol (rather than, e.g., a high-boiling diol), a simple reaction system under atmospheric pressure was employed to prevent the monomer and oligomers from climbing (Figure 2).

Figure 2. Designed polycondensation system under atmospheric pressure.

In this system, toluene forces the released methanol to evaporate and encounters the molecular sieves that were packed over the reaction flask to trap the methanol. Some toluene returns to the reaction flask and thus prevents the monomer and cyclic oligomer from climbing the flask walls. Due to the high reaction temperature, only a small portion of

the toluene is present in the flask at any time. While the reaction time used was longer than in the comparable vacuum polycondensation, the current method is operationally very simple. The molecular sieves can also be recycled after drying. The measured intrinsic viscosity of the prepared polyester was 0.22 dL/g. Figure 3 demonstrates the fundamental differences between the used polymerization techniques.

In another trial, a vacuum step (3 mbar pressure) was introduced after polycondensation under atmospheric pressure, when less oligomer should remain available for evaporation. Unexpectedly, the polymer produced by this method was very fragile and had a viscosity of 0.16 dL/g. Reduced molecular weight and hence viscosity often tend to result after some optimum reaction time is exceeded in high-temperature polycondensation of, e.g., PEF.[27,28] Considering that reversible polycondensations should have very high conversions to reach high molecular weights, small amounts of chain defects (e.g., etherification or decarboxylation) may also drastically limit the molecular weight.

Structural Characterization. The structure of pMSF was validated by ^{1}H and ^{13}C NMR analyses and comparisons against MSF (Figure 4). In ^{1}H NMR, the two sets of doublets (a and b) in the range of 6.5−7.5 ppm are assigned to the furan ring protons in both the monomer and the polymer. The aliphatic chain protons of pMSF (c and d) are detected at higher chemical shifts than in MSF. Only residual methyl ester and hydroxyl peaks (f and e, respectively) could be observed arising from the chain ends (Figure S5). The degree of polymerization estimated from their integrals was ca. 100. ^{13}C NMR spectra of MSF and pMSF were very similar apart from the absence of the methyl group peak in the pMSF spectrum. The most notable changes occurred in the chemical shifts of the carbons associated with the ethylene unit. In conclusion, the NMR results clearly showed that the desired self-condensed polyester was obtained from MSF and that a relatively high degree of polymerization was reached.

Depolymerization of pMSF. Depolymerization is becoming more important when designing or evaluating biobased polymers. The pMSF homopolyester could be depolymerized into MSF via a solvolysis procedure using K_2CO_3 and a solvent mixture of methanol and dichloromethane (Scheme 1). In contrast to the reported study on PET depolymerization,[24] the pMSF specimens were not completely disintegrated at 25 °C using a methanol/dichloromethane mixture for 24 h. Based on ^{1}H NMR (Figure S6a), that chemical recycling approach was unsuccessful, and a higher temperature was required to achieve full depolymerization: Employing a reaction temperature of 50 °C while using the same solvent mixture facilitated the almost complete recovery of MSF (97% yield) over 1 day reaction time (Figure S6b). If only methanol was used instead of methanol/dichloromethane mixture, a lower yield of MSF was obtained (79%) due to partial hydrolysis (Figure S7a,b). In a hypothetical scenario, the chemical recycling process of pMSF from mixed plastic streams, which may include materials such as PET, holds the promise of being straightforward and direct. Physical segregation of mixed polymer waste might not be necessary as a preliminary step before chemical recycling procedures. This consideration arises from the dissimilarity in physical attributes between the recovered MSF and other monomers, such as dimethyl terephthalate and ethylene glycol. The fact that the recovered MSF monomer is denser than liquid water implies a tendency for phase segregation in, e.g., aqueous conditions. Under similar conditions, typical diols
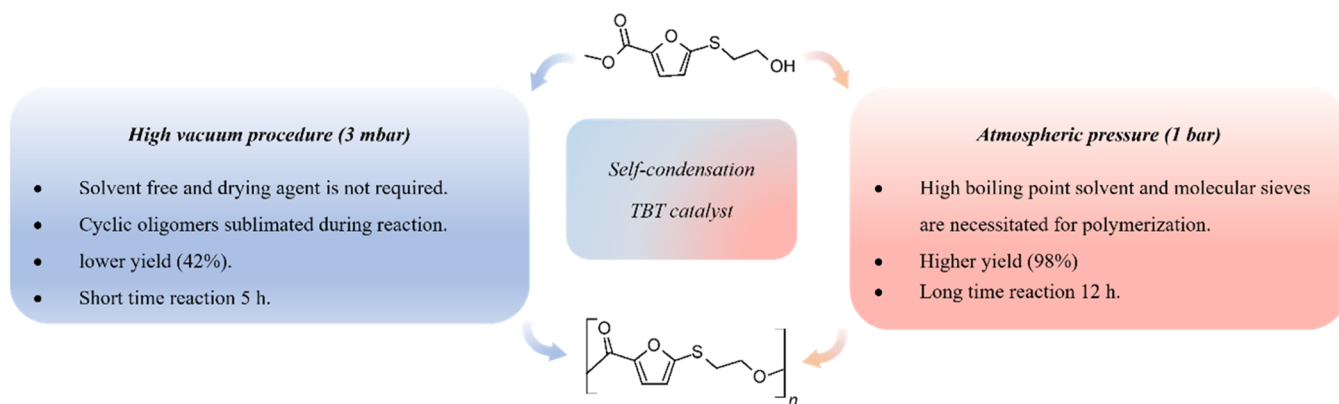
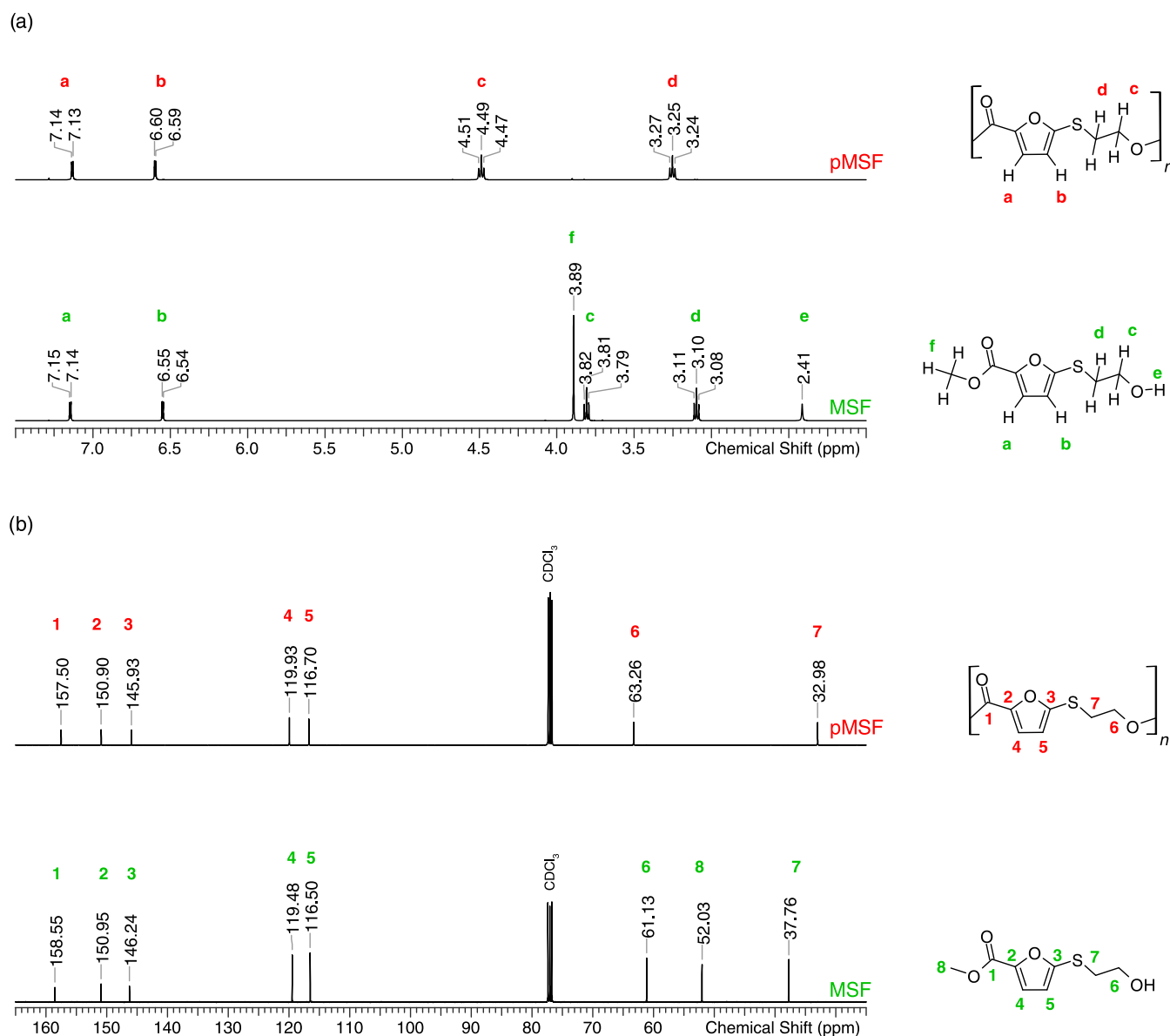**Figure 3.** Differences between the applied polymerization techniques.

Figure 4. Signal assignments of pMSF and MSF in CDCl$_3$. (a) ^{1}H NMR (2–8 ppm) and (b) ^{13}C NMR (20–170 ppm).

such as ethylene glycol would remain in a dissolved state within the aqueous medium. Conversely, dimethyl terephthalate would predominantly crystallize into solid forms that could be collected through filtration. MSF itself can also be separated and purified further by vacuum distillation, if necessary. This hypothesis underscores the potential viability of a closed-loop chemical recycling approach for pMSF.
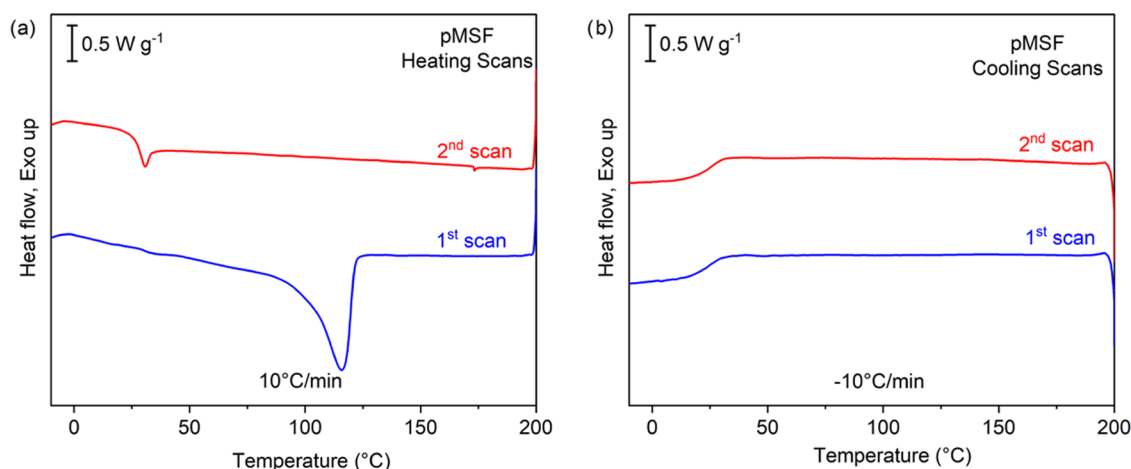
Figure 5. DSC (a) heating scans and (b) cooling scans of pMSF.

Further investigations are required to substantiate this hypothesis.

Thermal Characterization. The DSC heating and cooling curves of pMSF are shown in Figure 5, and the thermal properties are summarized in Table 1. The presence of the

Table 1. Thermal Properties of pMSF Compared to PESF and PEF[a]

| | DSC | | TGA | | | | |
| | | | N$_2$ | | | air | |
sample	T_g (°C)	T_m (°C)	T_{d5} (°C)	T_{d50} (°C)	R_{700} (%)	T_{d5} (°C)	T_{d50} (°C)
pMSF	25	120	329	354	23.6	320	361
PESF[b]	65	164	363	383	23.2	352	376
PEF[c]	85	210	354	411	12.5	360	415

[a]T_g: Glass transition temperature from 2nd cooling. T_m: Melting temperature from 1st heating. T_{d5}: Temperature at 5% sample mass-loss. T_{d50}: Temperature at 50% sample mass-loss. R_{700}: Residual mass at 700 °C. nd: not detected. [b]Ref 16. [c]Ref 26.

sulfur bridge between the ethylene chain and the furan ring reduces chain rigidity, enhances ductility, and hence remarkably decreases the T_g to 25 °C. This value is much lower than those of the structurally related polyesters PESF and PEF, with glass transition temperatures of 65 and of 85 °C,

respectively.[16,26] An endothermic peak from polymer melting was observed in the first heating scan at 120 °C, which appears to result from solvent crystallization due to the precipitation in methanol. We found that although pMSF is soluble in chloroform under a slightly elevated temperature (40 °C), it only slightly dissolves in cold chloroform before turning white due to crystallization (e.g., amorphous film form). Similarly, crystallization occurs if chloroform is simply allowed to evaporate from the solution. Crystallization or melting was not observed after the initial measurement. A similar amorphous character was previously found for the sulfur-bridged difuran polyesters such as PESF, even though they have a more symmetric structure than pMSF. While pMSF has a low T_g close to room temperature and very little crystallinity, free-standing films were readily obtained to allow further characterization.

The thermal degradation behavior and stability of pMSF were assessed by TGA (Table 1 and Figure 6). The onset (T_{d5}) and degradation temperatures (T_{d50}) under N$_2$ atmosphere were 329 and 354 °C, respectively, indicating that pMSF is clearly thermally stable under melt processing conditions (T_m = 120 °C). When compared to PEF and PESF, the alkyl sulfide-type structure does slightly lower thermal stability. The char residue of pMSF at 700 °C was 23.6%, close to that of PESF and higher than that of PEF. For further
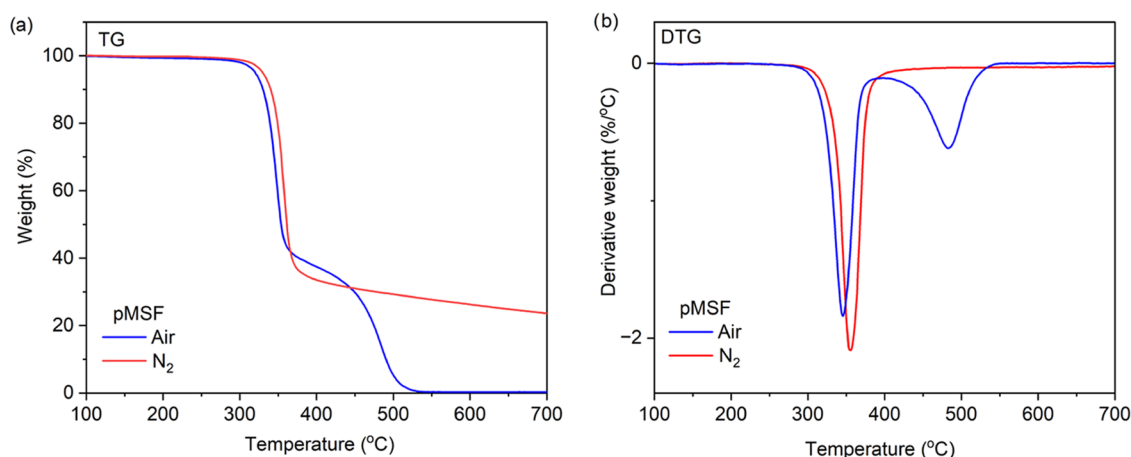

Figure 6. (a) TG and (b) DTG of pMSF under air and N$_2$.

investigation, pMSF degradation was analyzed under air conditions, which was significantly different from that under N_2: Two stages of weight loss occurred, and an earlier onset of decomposition was observed. pMSF first degraded at 320 °C in the major decomposition step, while the resultant char residue was burned off in the minor step in the range of 361−520 °C, which was comparable to PESF.

Thermomechanical and Mechanical Characterization. The relevant tensile properties of the pMSF film, i.e., tensile modulus (E_t), maximum tensile stress (σ_m), and elongation at break (ε_b), are presented in Table 2. pMSF samples had lower

Table 2. Measured Tensile Properties of the pMSF Specimens[a]

sample	E_t (MPa)	σ_m (MPa)	ε_b (%)
pMSF	394 ± 86	2.6 ± 0.8	586 ± 143
PESF[b]	2560 ± 300	52 ± 5	2.3 ± 0.5
PEF[c]	2752 ± 186	65 ± 6	4 ± 0.66

[a]At least five amorphous specimens were evaluated. E_t = Tensile modulus. σ_m = Maximum tensile stress. ε_b = Elongation at break. [b]Ref 16. [c]Ref 26.

modulus and strength than PESF and PEF, but a significantly higher elongation at break of 586%, which makes it ideal for applications requiring high elongation. A stress−strain curve of a representative specimen is shown in Figure S8. Interestingly, pMSF shows the typical elastomeric response, i.e., the absence of yielding and almost complete recovery after deformation. On this basis, we were encouraged to study the elastic deformation behavior of pMSF. A polyester specimen was deformed using a strain of 200% and maintained for 1 min to ensure the temporary deformation under stable conditions of 23 °C and 50% RH. Subsequently, the specimen was allowed to return to its shape after releasing the external stress. Within the first minute, elastic behavior was observed, and the sample shrunk to about 160% of its original length. The sample almost returns to the original length after 2-day recovery (ca. 107% of the original) (Figure S9). There was no further change observed in the length of the specimen after storing for 1 week. The elastic behavior of pMSF demonstrates the potential for packaging applications where stretchability is demanded.

For further characterization of pMSF, dynamic mechanical analysis (DMA) was performed. Figure 7 illustrates how the glass transition corresponds to the softening of a material. The evaluated T_g values from the peak positions of loss modulus E''
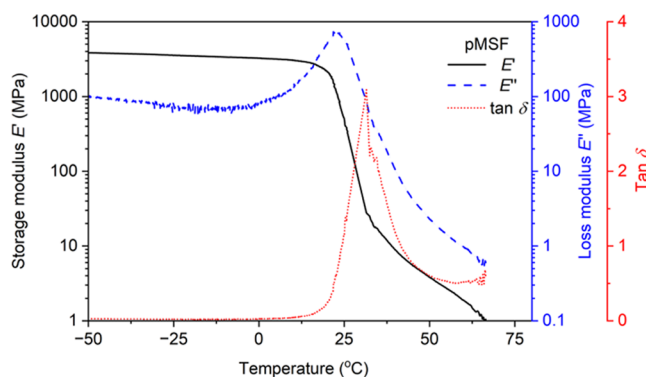

Figure 7. DMA thermogram for pMSF showing the storage modulus E', loss modulus E'', and tan δ as a function of temperature.

and tan δ were 23 and 30 °C, respectively. The value of the storage modulus (E') in the glassy state region was 3240 MPa at 0 °C, dramatically decreasing after 20 °C. The absence of cold crystallization and the immediate transition to viscous flow agreed with DSC results, emphasizing the amorphous character of pMSF.

Oxygen Barrier and UV Shielding Properties. From the perspective of packaging applications, developing polymeric materials for shelf-stable food packaging requires certain barrier properties, such as protection from oxygen permeation and UV light. As mentioned earlier, furan-based polymers are already well known for their low OP when compared against PET. For instance, PEF, PEBF, and PESF showed O_2 permeability reductions of 9.7×, 4.2×, and 11.2×, respectively.[15,16,26] Interestingly, the new biobased pMSF showed an O_2 gas transmission of up to 15× lower than amorphous PET (Table 3). This is interesting since low-T_g polyesters with low

Table 3. Permeability Properties of pMSF Compared to Other Polyesters

polymer	O_2 permeability		UV−light cutoff (nm)
	OP[a]	BIF[b]	
pMSF	0.0315	15.0	340
PESF[c]	0.0422	11.2	350
PEF[d]	0.0487	9.7	300
PEBF[e]	0.1100	4.2	400
PET[c]	0.4737	1	315

[a]Oxygen permeability in [cm^3 cm m^{-2} day^{-1} atm^{-1}] at 23 °C and 0% RH. [b]Calculated with a formula: BIF = OP$_{(PET)}$/OP$_{(Polyester)}$. [c]Ref 16. [d]Ref 26. [e]Refs 14,15.

oxygen gas permeability have scarcely been reported.[29] One such example is poly(pentylene furanoate) (PPeF), where depending on the film processing method, both very low O_2 permeabilities with a BIF value of over 200 and very high O_2 permeability with a BIF value as low as 0.26 have been reported.[30−32] The exceptional high barrier performance was attributed to the formation of highly ordered two-dimensional phase induced by the compression molding process, i.e., mesophase.[30,31] With pMSF, we did not observe any notable sensitivity with the O_2 barrier performance related to compression processing. Considering that the T_g of pMSF can be below the ambient temperature under some conditions, the permeability of the O_2 gas was also measured at 30 °C: Even above its T_g, pMSF had 6.3× lower permeability than amorphous PET.

We tested the O_2 permeability of pMSF film samples both directly after melt-pressing and after a period of storage at ambient conditions. A reasonable improvement was observed after a period of a few months, which may be attributed to the influence of physical aging and related structural effects on the free volume and chain packing of the polymer.[33] Further storage did not lower these final permeability values. As a conclusion, pMSF offers new possibilities for packaging applications where high oxygen barrier properties are requested.

Next, the light transmittance properties of the pMSF film were evaluated in the range of 200−800 nm. The UV−vis cutoff values (in nm) of pMSF, other furan-based polyesters, and PET are listed in Table 3. pMSF showed performance similar to the sulfur-bridged difuran polyesters,[16] e.g., PESF, providing good UV light filtering ability up to 340 nm

wavelength (Figure 8a). The conclusion from this result is that the UV shielding property does not require a sulfur linkage
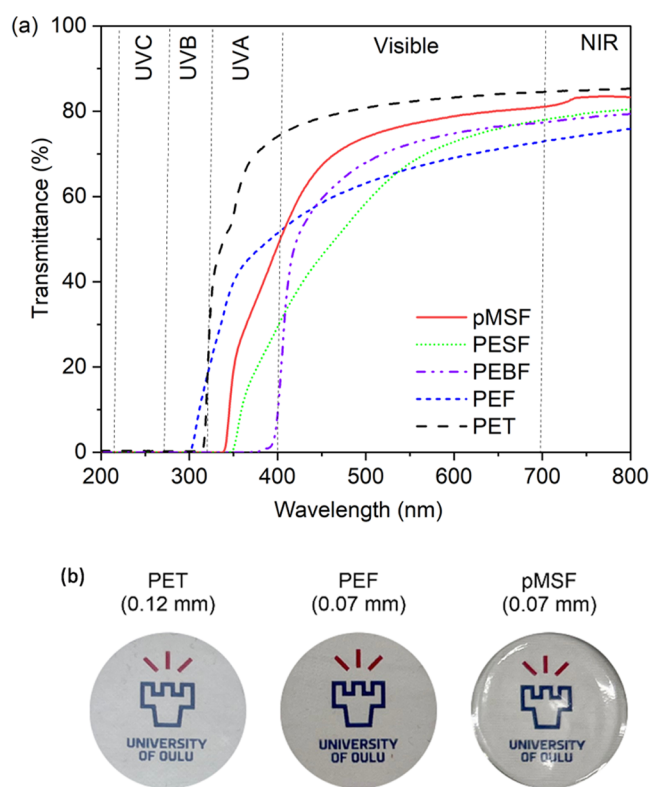

Figure 8. Optical properties of pMSF compared with related polymers: (a) UV−vis transmittance curves and (b) digital images over A4 printout.

between two furan rings but rather can be considered as a conjugated system formed by an electron-withdrawing carbonyl group connected to an electron-donating sulfur atom via the furan ring. In other words, the difuran sulfide moiety provides only a small enhancement in UV absorbance compared with the furan alkyl sulfide moiety of pMSF. Notably, pMSF showed a good balance between UV light filtering ability and transparency. Lignin-based additives, for example, often give polymers broad UV shielding but drastically decrease visual transparency.[34−36] In this context, the melt-pressed pMSF film exhibited a low degree of discoloration coupled with a high level of optical transparency, reaching up to 80% (Figure 8b). From, e.g., the packaging sector perspective, transparency and color clarity hold importance, particularly when aiming to replace or compete with a well-established product such as PET. The issues of discoloration related to furan-based polymers and the impact of utilized catalysts have been recognized in the literature.[37,38] The good visual appearance of pMSF is therefore encouraging, and exploring alternative polymerization catalysts or the incorporation of antioxidant additives could potentially offer a means to further improve the appearance. Given these findings, pMSF appears to be a promising polyester for stretchable packing applications with beneficial UV and oxygen gas barrier properties.

Copolymerization with PEF and PEBF. Encouraged by the results presented above, we also decided to demonstrate the use of MSF as a comonomer. The biobased dm-FDCA and its bifuran analogue, dm-BFDCA, were copolymerized with MSF to obtain two copolymers, $PEF_{80}MSF_{20}$ and $PEBF_{80}MSF_{20}$.

Both copolymers were synthesized using 4:1 molar ratios of the dimethyl ester monomer and MSF, respectively. A traditional two-step melt esterification and polycondensation process was used to prepare the targeted copolyesters with yields of 90% and 93%, respectively (Scheme S1). The measured IV values of the resulting copolymers were close to 0.4 dL/g or almost double that of pMSF. Based on NMR characterization (Figures S10−S13) and (Scheme S2), it was concluded that copolyesters with comonomer ratios close to the feed ratios were obtained. The copolymers could be efficiently chemically recycled as well, i.e., converted back to their corresponding monomers (Figures S14−S15). The DSC traces of the synthesized copolymers are presented in Figure S16. The recorded T_g values of $PEF_{80}MSF_{20}$ and $PEBF_{80}MSF_{20}$ were 66 and 89 °C, respectively, falling in line with the theoretical calculated values (Table S1). Both T_g values were lower than those in the respective homopolyesters, PEF and PEBF, because of the incorporation of the flexible MSF unit into the polymer chains. The 20 mol % MSF comonomer amount was sufficient to reduce the crystallinity of the resulting copolyesters, i.e., $PEF_{80}MSF_{20}$ and $PEBF_{80}MSF_{20}$ were highly amorphous polymers. Based on TGA results (Table S1 and Figure S17), the prepared copolyesters exhibited thermal degradation temperatures in the range of 350−370 °C under N_2, which fell in the same range as the values of PEF and PEBF. The mechanical properties were studied as well, and results are collected in Table S2. The synthesized copolymer showed a similar high tensile modulus of 2450 and 2310 MPa for $PEF_{80}MSF_{20}$ and $PEBF_{80}MSF_{20}$, respectively, as homopolyesters PEF and PEBF. The elongation, however, was highly limited by FDCA and BFDCA motifs. The results of DMA measurements agreed with DSC and confirmed the amorphous character of the prepared copolymers (Figure S18). In terms of the O_2 permeability, $PEF_{80}MSF_{20}$ and $PEBF_{80}MSF_{20}$ showed reduced oxygen permeabilities with respect to their neat homopolymers PEF and PEBF (Table S3). The evaluated BIF values were 11.8 and 5.6, respectively, compared to PET. Regarding UV filtering ability, $PEF_{80}MSF_{20}$ showed wavelength cutoff at 340 nm similar to pMSF, whereas $PEBF_{80}MSF_{20}$ showed increased UV filtering ability up to 380 nm due to BFDCA units present (Figure S19). In summary, the new MSF monomer can be used for modification polyesters affording better oxygen barrier performance and UV filtering ability.

■ CONCLUSIONS

A new furfural-derived biobased monomer MSF and its homopolyester pMSF were synthesized and characterized. A simple reaction system under atmospheric pressure was employed to prepare pMSF. The homopolyester displayed excellent chemical recyclability to regenerate the self-condensable monomer with high purity. Thanks to the introduction of the C−S linkage, the pMSF film exhibited good O_2 barrier performance, roughly 15× better than amorphous PET. This was combined with UV light filtering ability up to 340 nm. pMSF was measured to have a T_g of 25 °C and good thermal stability with decomposition taking place in the range 329−320 °C. Moreover, MSF could be utilized as a comonomer for improving the barrier properties of PEF and PEBF as well. The incorporation of 20 mol % of pMSF into the resulting copolyesters, i.e., $PEF_{80}MSF_{20}$ and $PEBF_{80}MSF_{20}$, was sufficient to noticeably reduce the O_2 permeability, enhance UV light cutoff, and reduce crystallinity. These results imply

that the new biobased pMSF has an appropriate potential as a flexible recyclable packing material with good gas barrier properties and UV filtering ability.

ASSOCIATED CONTENT

Supporting Information

The Supporting Information is available free of charge at https://pubs.acs.org/doi/10.1021/acs.macromol.3c01342.

> Characterization data of the synthesized monomer (Figures S1–S3); digital image and ^{1}H NMR spectrum of sublimated product under vacuum polycondensation (Figure S4); ^{1}H NMR spectra of recovered monomer (Figures S6 and S7); and mechanical characterization of pMSF (Figures S8 and S9); synthesis and structural characterization of copolymers (Schemes S1 and S2) and (Figures S10–S13); ^{1}H NMR spectra of recovered monomer mixtures (Figures S14 and S15); thermal properties (Table S1) and (Figures S16 and S17); mechanical properties (Table S2 and Figure S18); and permeability measurements (Table S3 and Figure S19) (PDF)

AUTHOR INFORMATION

Corresponding Author

Juha P. Heiskanen − *Research Unit of Sustainable Chemistry, University of Oulu, FI-90014 Oulu, Finland;* orcid.org/0000-0002-1884-1583; Email: juha.heiskanen@oulu.fi

Authors

Asmaa M. Ahmed − *Research Unit of Sustainable Chemistry, University of Oulu, FI-90014 Oulu, Finland;* orcid.org/0000-0001-8218-2909

Tuomo P. Kainulainen − *Research Unit of Sustainable Chemistry, University of Oulu, FI-90014 Oulu, Finland;* orcid.org/0000-0001-7027-8209

Juho Antti Sirviö − *Fibre and Particle Engineering Research Unit, University of Oulu, FI-90014 Oulu, Finland;* orcid.org/0000-0002-7404-3340

Complete contact information is available at:
https://pubs.acs.org/10.1021/acs.macromol.3c01342

Author Contributions

The manuscript was written through the contributions of all authors.

Notes

The authors declare no competing financial interest.

ACKNOWLEDGMENTS

REFERENCES

(1) Gandini, A. Furans as Offspring of Sugars and Polysaccharides and Progenitors of a Family of Remarkable Polymers: A Review of Recent Progress. *Polym. Chem.* **2010**, *1* (3), 245−251.

(2) Zhang, D.; Dumont, M. J. Advances in Polymer Precursors and Bio-Based Polymers Synthesized from 5-Hydroxymethylfurfural. *J. Polym. Sci., Part A: Polym. Chem.* **2017**, *55* (9), 1478−1492.

(3) Gandini, A.; M Lacerda, T. Furan Polymers: State of the Art and Perspectives. *Macromol. Mater. Eng.* **2022**, *307* (6), No. 2100902.

(4) de Jong, E.; Visser, H. R. A.; Dias, A. S.; Harvey, C.; Gruter, G.-J. M. The Road to Bring FDCA and PEF to the Market. *Polymers* **2022**, *14* (5), 943.

(5) Loos, K.; Zhang, R.; Pereira, I.; Agostinho, B.; Hu, H.; Maniar, D.; Sbirrazzuoli, N.; Silvestre, A. J. D.; Guigo, N.; Sousa, A. F. A Perspective on PEF Synthesis, Properties, and End-Life. *Front. Chem.* **2020**, *8*, No. 585.

(6) Papageorgiou, G. Z.; Papageorgiou, D. G.; Terzopoulou, Z.; Bikiaris, D. N. Production of Bio-Based 2,5-Furan Dicarboxylate Polyesters: Recent Progress and Critical Aspects in Their Synthesis and Thermal Properties. *Eur. Polym. J.* **2016**, *83*, 202−229.

(7) Burgess, S. K.; Karvan, O.; Johnson, J. R.; Kriegel, R. M.; Koros, W. J. Oxygen Sorption and Transport in Amorphous Poly(Ethylene Furanoate). *Polymer* **2014**, *55* (18), 4748−4756.

(8) Burgess, S. K.; Kriegel, R. M.; Koros, W. J. Carbon Dioxide Sorption and Transport in Amorphous Poly(Ethylene Furanoate). *Macromolecules* **2015**, *48* (7), 2184−2193.

(9) Burgess, S. K.; Leisen, J. E.; Kraftschik, B. E.; Mubarak, C. R.; Kriegel, R. M.; Koros, W. J. Chain Mobility, Thermal, and Mechanical Properties of Poly(Ethylene Furanoate) Compared to Poly(Ethylene Terephthalate). *Macromolecules* **2014**, *47* (4), 1383−1391.

(10) Araujo, C. F.; Nolasco, M. M.; Ribeiro-Claro, P. J. A.; Rudić, S.; Silvestre, A. J. D.; Vaz, P. D.; Sousa, A. F. Inside PEF: Chain Conformation and Dynamics in Crystalline and Amorphous Domains. *Macromolecules* **2018**, *51* (9), 3515−3526.

(11) Lei, Y.; Zhang, S.; Shen, G.; Zhu, J.; Xue, J.; Chen, Z.; Yin, G. Feasible Synthesis of a Bifuran-Based Monomer for Polymer Synthesis from a Hemicellulose-Derived Platform. *Ind. Eng. Chem. Res.* **2020**, *59*, 19876−19883.

(12) Miyagawa, N.; Ogura, T.; Okano, K.; Matsumoto, T.; Nishino, T.; Mori, A. Preparation of Furan Dimer-Based Biopolyester Showing High Melting Points. *Chem. Lett.* **2017**, *46* (10), 1535−1538.

(13) Miyagawa, N.; Suzuki, T.; Okano, K.; Matsumoto, T.; Nishino, T.; Mori, A. Synthesis of Furan Dimer-Based Polyamides with a High Melting Point. *J. Polym. Sci., Part A: Polym. Chem.* **2018**, *56* (14), 1516−1519.

(14) Kainulainen, T. P.; Sirviö, J. A.; Sethi, J.; Hukka, T. I.; Heiskanen, J. P. UV-Blocking Synthetic Biopolymer from Biomass-Based Bifuran Diester and Ethylene Glycol. *Macromolecules* **2018**, *51* (5), 1822−1829.

(15) Edling, H. E.; Sun, H.; Paschke, E.; Schiraldi, D. A.; Tanko, J. M.; Paradzinsky, M.; Turner, S. R. High Barrier Biosourced Polyester from Dimethyl [2,2′-Bifuran]-5,5′-Dicarboxylate. *Polymer* **2020**, *191*, No. 122258.

(16) Ahmed, A. M.; Kainulainen, T. P.; Sirviö, J. A.; Heiskanen, J. P. Renewable Furfural-Based Polyesters Bearing Sulfur-Bridged Difuran Moieties with High Oxygen Barrier Properties. *Biomacromolecules* **2022**, *23* (4), 1803−1811.

(17) Li, L.-G.; Wang, Q.-Y.; Zheng, Q.-Y.; Du, F.-S.; Li, Z.-C. Tough and Thermally Recyclable Semiaromatic Polyesters by Ring-Opening Polymerization of Benzo-Thia-Caprolactones. *Macromolecules* **2021**, *54* (14), 6745−6752.

(18) Mialon, L.; Vanderhenst, R.; Pemba, A. G.; Miller, S. A. Polyalkylenehydroxybenzoates (PAHBs): Biorenewable Aromatic/Aliphatic Polyesters from Lignin. *Macromol. Rapid Commun.* **2011**, *32* (17), 1386−1392.

(19) MacDonald, J. P.; Shaver, M. P. An Aromatic/Aliphatic Polyester Prepared via Ring-Opening Polymerisation and Its Remarkably Selective and Cyclable Depolymerisation to Monomer. *Polym. Chem.* **2016**, *7* (3), 553−559.

(20) Lizundia, E.; Makwana, V. A.; Larrañaga, A.; Vilas, J. L.; Shaver, M. P. Thermal, Structural and Degradation Properties of an Aromatic−Aliphatic Polyester Built through Ring-Opening Polymerisation. *Polym. Chem.* **2017**, *8* (22), 3530−3538.

(21) Fan, H.-Z.; Yang, X.; Wu, Y.-C.; Cao, Q.; Cai, Z.; Zhu, J.-B. Leveraging the Monomer Structure for High-Performance Chemically Recyclable Semiaromatic Polyesters. *Polym. Chem.* **2023**, *14* (6), 747−753.

(22) Kainulainen, T. P.; Hukka, T. I.; Özeren, H. D.; Sirviö, J. A.; Hedenqvist, M. S.; Heiskanen, J. P. Utilizing Furfural-Based Bifuran Diester as Monomer and Comonomer for High-Performance Bioplastics: Properties of Poly(Butylene Furanoate), Poly(Butylene Bifuranoate), and Their Copolyesters. *Biomacromolecules* **2020**, *21* (2), 743−752.

(23) Kainulainen, T. P.; Parviainen, T. A. O.; Sirviö, J. A.; McGeachie, L. J. R.; Heiskanen, J. P. High Oxygen Barrier Polyester from 3,3′-Bifuran-5,5′-Dicarboxylic Acid. *ACS Macro Lett.* **2023**, *12* (2), 147−151.

(24) Pham, D. D.; Cho, J. Low-Energy Catalytic Methanolysis of Poly(Ethyleneterephthalate). *Green Chem.* **2021**, *23* (1), 511−525.

(25) Billmeyer, F. W., Jr. Methods for Estimating Intrinsic Viscosity. *J. Polym. Sci.* **1949**, *4* (1), 83−86.

(26) Ahmed, A. M.; Kainulainen, T. P.; Sirviö, J. A.; Heiskanen, J. P. High-Barrier Biobased Copolyesters with Targeted Glass Transition Temperatures as Renewable Alternatives for PET. *ACS Appl. Polym. Mater.* **2023**, *5* (3), 2144−2153.

(27) Yu, Z.; Zhou, J.; Cao, F.; Zhang, Q.; Huang, K.; Wei, P. Synthesis, Characterization and Thermal Properties of Bio-Based Poly(Ethylene 2,5-Furan Dicarboxylate). *J. Macromol. Sci., Part B* **2016**, *55* (12), 1135−1145.

(28) Terzopoulou, Z.; Karakatsianopoulou, E.; Kasmi, N.; Tsanaktsis, V.; Nikolaidis, N.; Kostoglou, M.; Papageorgiou, G. Z.; Lambropoulou, D. A.; Bikiaris, D. N. Effect of Catalyst Type on Molecular Weight Increase and Coloration of Poly(Ethylene Furanoate) Biobased Polyester during Melt Polycondensation. *Polym. Chem.* **2017**, *8* (44), 6895−6908.

(29) Bianchi, E.; Soccio, M.; Siracusa, V.; Gazzano, M.; Thiyagarajan, S.; Lotti, N. Poly(Butylene 2,4-Furanoate), an Added Member to the Class of Smart Furan-Based Polyesters for Sustainable Packaging: Structural Isomerism as a Key to Tune the Final Properties. *ACS Sustainable Chem. Eng.* **2021**, *9* (35), 11937−11949.

(30) Guidotti, G.; Soccio, M.; García-Gutiérrez, M.-C.; Gutiérrez-Fernández, E.; Ezquerra, T. A.; Siracusa, V.; Munari, A.; Lotti, N. Evidence of a 2D-Ordered Structure in Biobased Poly-(Pentamethylene Furanoate) Responsible for Its Outstanding Barrier and Mechanical Properties. *ACS Sustainable Chem. Eng.* **2019**, *7* (21), 17863−17871.

(31) Guidotti, G.; Soccio, M.; García-Gutiérrez, M. C.; Ezquerra, T.; Siracusa, V.; Gutiérrez-Fernández, E.; Munari, A.; Lotti, N. Fully Biobased Superpolymers of 2,5-Furandicarboxylic Acid with Different Functional Properties: From Rigid to Flexible, High Performant Packaging Materials. *ACS Sustainable Chem. Eng.* **2020**, *8* (25), 9558−9568.

(32) Xie, H.; Wu, L.; Li, B. G.; Dubois, P. Modification of Poly(Ethylene 2,5-Furandicarboxylate) with Biobased 1,5-Pentanediol: Significantly Toughened Copolyesters Retaining High Tensile Strength and O₂ Barrier Property. *Biomacromolecules* **2019**, *20* (1), 353−364.

(33) *Polymer Blends Handbook*, 2nd ed.; Utracki, L. A.; Wilkie, C. A., Eds.; Springer: New York, 2014.

(34) Zhang, X.; Liu, W.; Yang, D.; Qiu, X. Biomimetic Supertough and Strong Biodegradable Polymeric Materials with Improved Thermal Properties and Excellent UV-Blocking Performance. *Adv. Funct. Mater.* **2019**, *29* (4), No. 1806912.

(35) Kim, Y.; Suhr, J.; Seo, H.-W.; Sun, H.; Kim, S.; Park, I.-K.; Kim, S.-H.; Lee, Y.; Kim, K.-J.; Nam, J.-D. All Biomass and UV Protective Composite Composed of Compatibilized Lignin and Poly (Lactic-Acid). *Sci. Rep.* **2017**, *7* (1), No. 43596.

(36) Zhang, Y.; Zhou, S.; Fang, X.; Zhou, X.; Wang, J.; Bai, F.; Peng, S. Renewable and Flexible UV-Blocking Film from Poly(Butylene Succinate) and Lignin. *Eur. Polym. J.* **2019**, *116*, 265−274.

(37) Sousa, A. F.; Patrício, R.; Terzopoulou, Z.; Bikiaris, D. N.; Stern, T.; Wenger, J.; Loos, K.; Lotti, N.; Siracusa, V.; Szymczyk, A.; Paszkiewicz, S.; Triantafyllidis, K. S.; Zamboulis, A.; Nikolic, M. S.; Spasojevic, P.; Thiyagarajan, S.; van Es, D. S.; Guigo, N. Recommendations for Replacing PET on Packaging, Fiber, and Film Materials with Biobased Counterparts. *Green Chem.* **2021**, *23* (22), 8795−8820.

(38) Banella, M. B.; Bonucci, J.; Vannini, M.; Marchese, P.; Lorenzetti, C.; Celli, A. Insights into the Synthesis of Poly(Ethylene 2,5-Furandicarboxylate) from 2,5-Furandicarboxylic Acid: Steps toward Environmental and Food Safety Excellence in Packaging Applications. *Ind. Eng. Chem. Res.* **2019**, *58* (21), 8955−8962.

📖 **Recommended by ACS**